JMEPEG (2005) 14:37-49
DOI: 10.1361/10599490522239

1059-9495/$19.00

Role of the Cyclic Stability of Retained Austenite in Fatigue Performance of Carburized 14NiCr11 Steel

Dalenda Jeddi, Habib Sidhom, Dominique Ghiglione, and Henri-Paul Lieurade

(Submitted February 20, 2004)

The role of retained austenite in the fatigue strength of carburized 14NiCr11 steel was studied by considering two gas-carburizing treatments leading to two maximum retained austenite fractions of 20 and 40%. These states led to endurance limit improvements evaluated at 40 and 10%, respectively, compared with the untreated state. These improvements were explained by the evolution of retained austenite during the cyclic loading using the dispersive x-ray diffraction technique. This reveals that the best fatigue strength is attributed to the homogeneous transformation of the retained austenite fraction in the treated layer during the cyclic loading.

Keywords carburizing, fatigue, residual stress, retained austenite, steel

1. Introduction

The improvement in fatigue strength for machine components manufactured with microalloyed steels is due to hardening treatments that offer a hardened layer over a ductile core (Ref 1-3). Among these treatments, carburizing, with its various forms (Ref 3-15), remains the most popular hardening treatment used for small and average sized parts manufactured from low-alloy steel with lower-to-modest mechanical properties (Ref 16). Hardened layers with thicknesses ranging from 0.5 mm to a few millimeters, and experiencing compressive residual stresses, can be achieved with a carburizing treatment. Carburized steel is also associated with retained austenite and martensite microstructures in proportions that depend on the carburizing conditions and the steel type (Ref 17-43). This change in microstructure improves the fatigue strength of the treated components by increasing the endurance limit or number of cycles to failure, as shown in Table 1. Existing literature attributes these improvements to the compressive residual stress distribution (Ref 1, 17, 44). The effect of the microstructural gradient, and especially that of retained austenite in the hardened layers, has not been studied extensively due to the lack of suitable and precise methods that would yield conclusive results (Ref 45), even though some work has been done (Ref 46-51). Indeed, Zaccone and Krauss (Ref 46) affirm that retained austenite decreases tensile properties such as fatigue

Dalenda Jeddi and **Habib Sidhom,** Laboratoire de Mécanique Matériaux et Procédés, 5 Av Taha Hussein, 1008 Tunis, Tunisie; and **Dominique Ghiglione** and **Henri-Paul Lieurade,** French Industrial and Mechanical Technical Centre, Senlis-France. Contact e-mail: Dalenda.Jeddi@ipeiem.rnu.tn.

Table 1 Influence of carburized layers characteristics on fatigue strength

	Treatment parameters				Structure characteristics			Test conditions				Result	
Steel grade	Type	T °C	t h	State	e (mm)	γ_R %	$\sigma_{R\ surf}$ (MPa)	Type	R	Run outs	K_t	σ_{Dmax} (MPa)	Ref
20CrMo4	Gas	900	…	QO 60°	0.6	35	−40	Bending 3 point	…	5×10^6	1	1465	62
	Gas	930	2	T 180°	0.58	17.1	+17	Rotating-bending	0.1	…	2	780	…
	LP	930	2	T 180°	0.61	15.4	−165	Rotating-bending		…	…	830	63
AISI8620	Gas	900	3	T 180°/1 h	0.73	37	−265	Rotating-bending	…	10^6	…	840	64
			5		0.90	49	−220				…	980	
			7.5	T180°/1 h	1.1	64	−200	Rotating-bending	…	10^6	…	1140	…
	Gas	940	2	QO Cryogenic + T 180°/2 h	…	0.5	…	Rotating-bending	…	10^7	…	735	…
				QO hot + T 180°/2 h	…	0.5	…	Rotating-bending	…	10^7	…	833	65

Note: Q, quenched; O, oil; T, tempered; LP, low-pressure carburizing treatment; R, $\sigma_{min}/\sigma_{max}$: stress ratio; K_t, stress concentration factor; σ_{Dmax}, endurance limit expressed in maximum stress

strength. They assume that the reduction in these properties is due to the thermodynamic instability of retained austenite under the effect of service stresses of hardened components. Other authors have tried to link the influence of retained austenite to its content in the hardened structure. Indeed, the results of the investigations of Krauss (Ref 24), Szpunar and Bielanik (Ref 20), Lesage and Iost (Ref 48), and Desalos (Ref 49) have indicated that the reduction in the fatigue strength of carburized components takes place when the retained austenite exceeds 15 to 20%. The experimental results obtained by Da Silva et al. (Ref 35), Prenosil (Ref 47), Parrish (Ref 22), Ebert (Ref 17), Panhans and Fournelle (Ref 25), Inada et al. (Ref 50), and Shaw et al. (Ref 51) have indicated that the presence of retained austenite in the case of carburized materials improves their ductility and fatigue strength.

However, the difficulty in controlling the evolution of this microstructural gradient during the cyclic loading and its effects on the fatigue strength remains an issue. This has been exclusively studied by Szpunar and Bielanik (Ref 20). They showed that for 18HGT and 20HNMh steels, the relation between the fatigue crack growth rate *da*/*dN* and retained austenite is very complicated.

It is within this framework that this research was undertaken, with the goal of elucidating the role of the microstructure gradient of the hardened layer during cyclic loading on

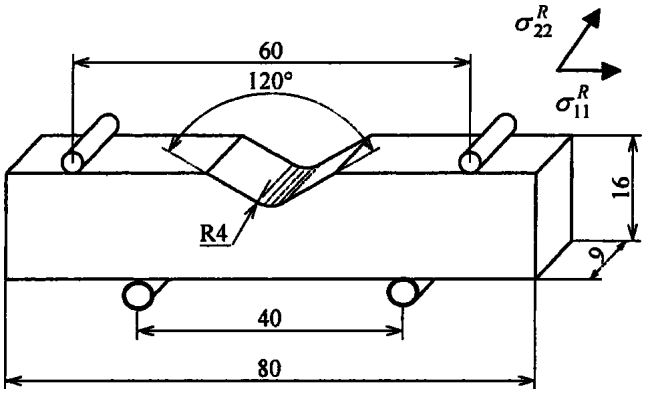

Fig. 1 Fatigue specimens and directions of residual stress measurement

Table 2 Chemical composition of 14NiCr11 steel

Composition, wt.%									
C	Si	Mn	P	S	Cr	Ni	Mo	Cu	Fe
0.14	0.24	0.46	0.015	0.032	0.79	3.18	<0.02	0.22	bal

Note: composition is in wt.%

Table 3 Traction characteristics

$R_{0.002}$, MPa	UTS, MPa	Elongation, %
408.6	553.6	30

Table 4 Parameters of gas-carburizing treatments

Type of treatment	Carbon potential	Carburizing temperature, °C	Time, h	Type of quench	Tempering treatment
Type 1	0.8	920	8	Oil 50 °C	180 °C, 1 h
Type 2	1.2	950	6	Oil 50 °C	180 °C, 1 h

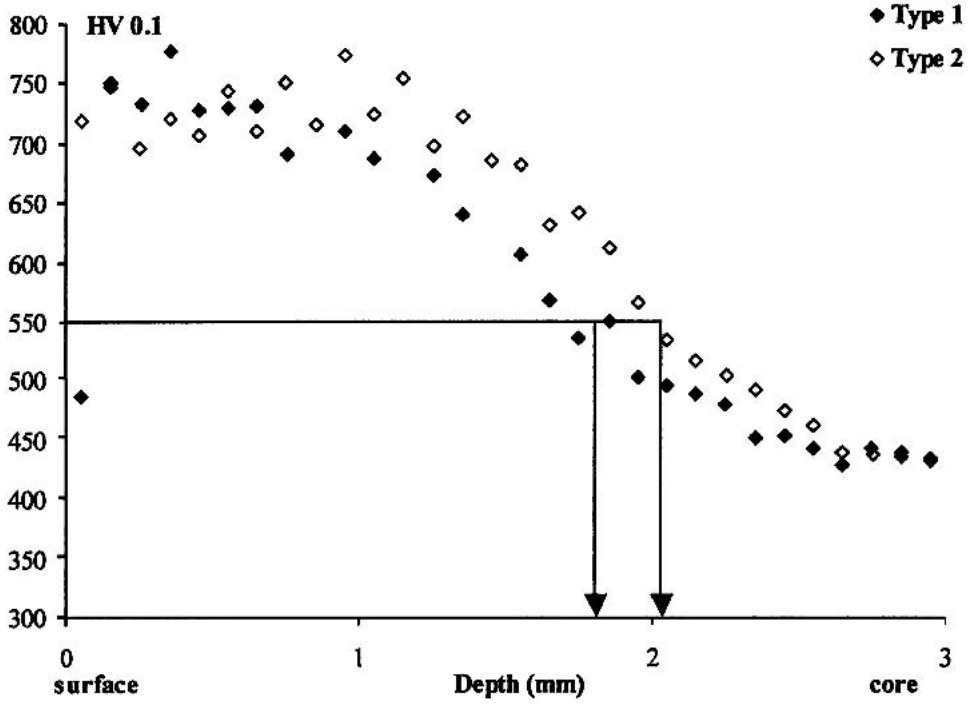

Fig. 2 Microhardness profiles resulting from the two types of carburizing 14NiCr11 steel

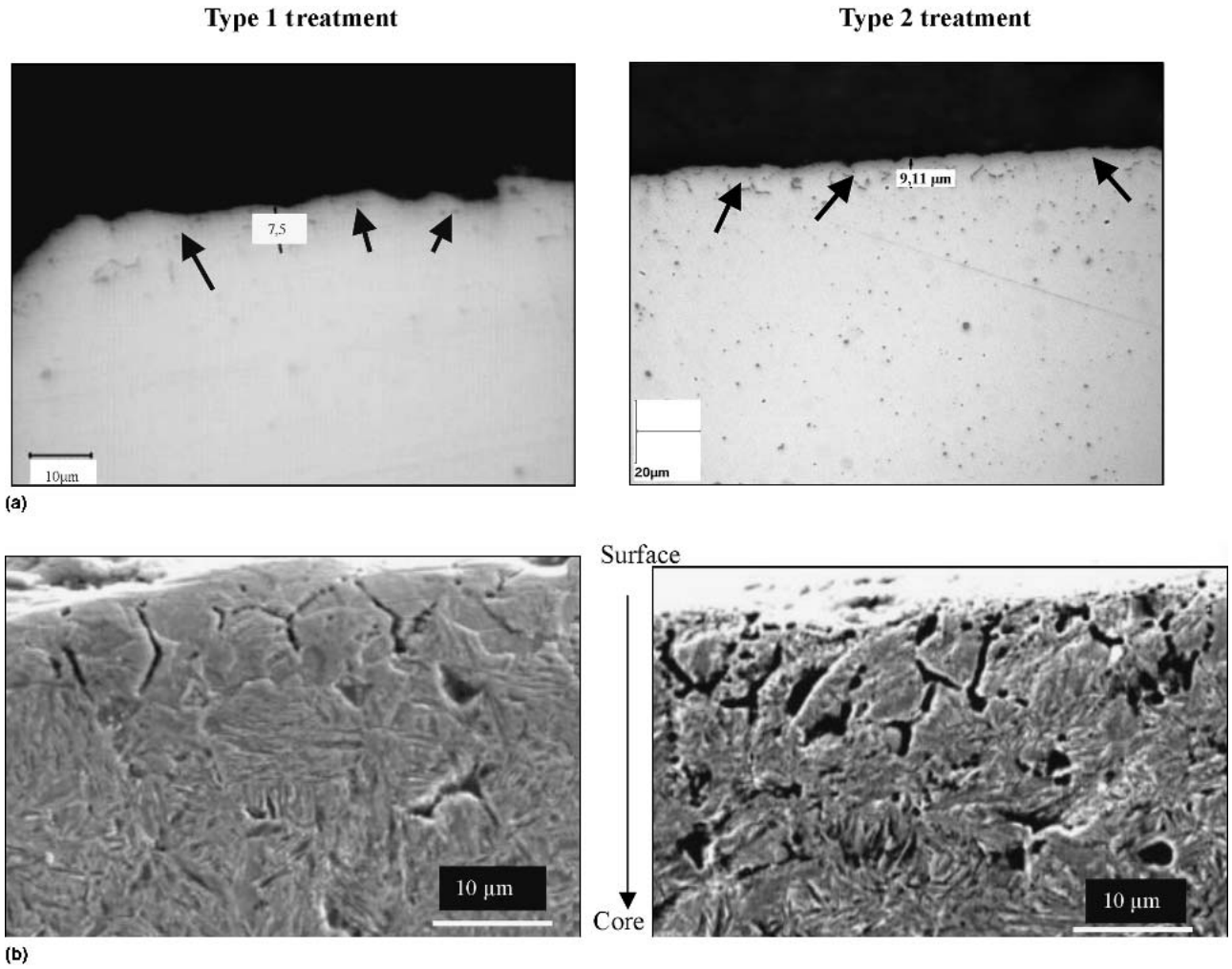

Fig. 3 Internal oxidation. (a) Internal oxidation on unetched surface. (b) Intergranular carbides in grain boundaries on surface upper layer

fatigue strength. Two conditions of gas carburizing are used on the 14NiCr11 steel leading to retained austenite volume fractions of 20 and 40%.

2. Material

The material used in this research was a low C steel, type 14NiCr11. The material was produced in 20 mm diam bars from the same cast. Its chemical composition and mechanical properties are shown in Tables 2 and 3, respectively.

3. Treatments and Tests

3.1 Carburizing Treatments

Two types of gas carburizing, aimed at achieving two fractions of retained austenite in the hardened layer, were applied to notched fatigue test samples stress concentration factor (K_T = 1.78) (Fig. 1). The selected notch is representative of gear tooth geometry (Ref 52-54). Treatment parameters are given in Table 4:

- The first type of treatment is representative of the conditions usually used in industry to limit the retained austenite fraction to 20% or lower for reasons of fatigue performance (Ref 20, 24, 45, 49).
- The second treatment aims to obtain a higher retained austenite fraction by choosing a higher C potential (i.e., 1.2 instead of 0.8) and a higher treatment temperature (i.e., 950 °C instead of 920 °C).

3.2 Characterization of Treated Layer Methods

3.2.1 Treated Layers Analysis. Surface hardening induced by the various carburizing treatments was evaluated by microhardness tests under a load of 100 g_f. The resulting metallurgical transformations were examined by optical microscopy (OM) and scanning electron microscopy (SEM) on transverse sections. The residual stress profiles were determined by x-ray diffraction (XRD). Retained austenite fractions were determined by XRD (Ref 55).

3.2.2 Fatigue Tests. Specimens were subjected to four-point bend fatigue tests with a 0.1 stress ratio value. Endurance limits were based on runouts to 10^6 cycles.

3.2.3 Microfractographic Analysis. The fracture surfaces were observed on the SEM images to determine the mechanisms that controlled fatigue crack initiation and propagation in relation to the characteristics of the treated layer, particularly the relation of retained austenite content to residual stress profiles.

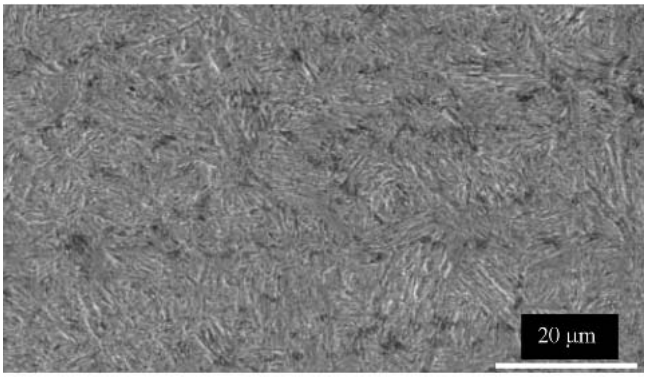

(a)

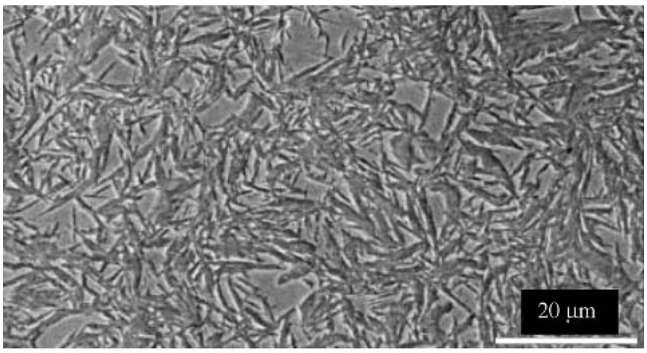

(b)

Fig. 4 Structure of carburized layer: needlelike martensite + retained austenite (at a depth of 200 μm from the upper surface)

4. Results

4.1 Hardness and Microstructure

Microhardness in direct line on transverse sections revealed a carburized depth of 1.8 mm for the type 1 treatment and 2 mm for the type 2 treatment (Fig. 2). These microhardness profiles were supplemented by metallographic analyses using OM and SEM. From the external surface toward the core, microscopy revealed:

- Internal oxidation on the upper surface that did not exceed 12 μm for both treatments: 8 μm for type 1 and 12 μm for type 2. The grain boundaries were decorated by intergranular precipitates (Fig. 3)
- A heterogeneous structure in the treated layer characterized by the presence of needlelike martensite and retained

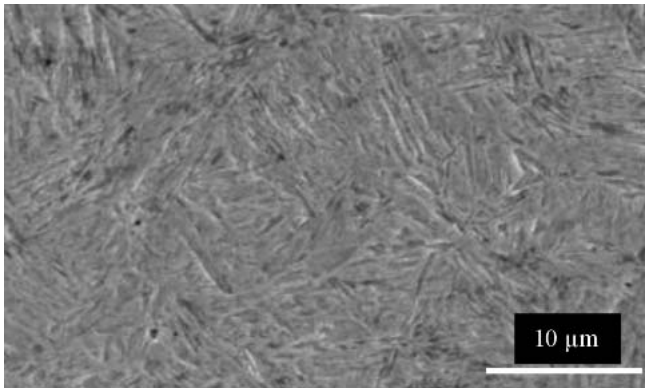

Fig. 5 Bainite structure in core

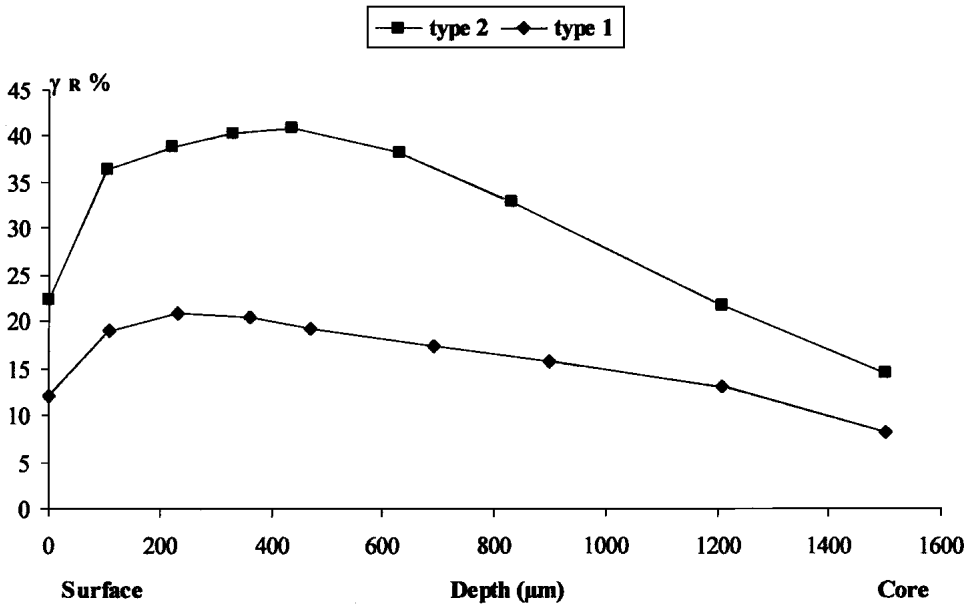

Fig. 6 Retained austenite profiles corresponding to the two types of treatment of 14NiCr11 steel

austenite with different aspects, as a result of the different retained austenite fractions (Fig. 4)
- A bainitic structure in the core (Fig. 5)

4.2 Retained Austenite

The retained austenite profiles measured at the bottom of the notch in the specimens (Fig. 6) showed that:

- At every point of the hardened layer, the amount of retained austenite obtained through the type 2 treatment was higher than that obtained by the type 1 treatment.
- The maximum retained austenite fractions of 20 and 40%, respectively, for type 1 and type 2 treatments were reached at a depth of 230 μm. This fraction is found to be almost constant at depths between 230 and 730 μm (or deeper).
- Near the surface, the retained austenite fraction decreases gradually to values of 12 and 22%, respectively, for type 1 and type 2 treatments (Fig. 6).

Surface measurements of retained austenite indicate a mild dispersion from 2 to 3% due to internal oxidation. In fact, with XRD measurement, the beam penetrates beyond the oxi-

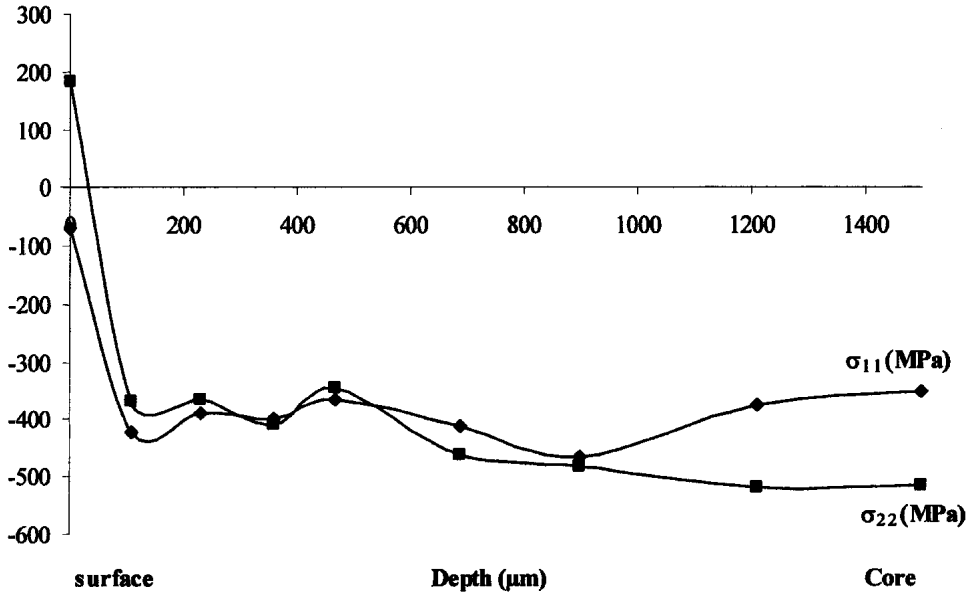

Fig. 7 Residual stress profiles generated by type 1 treatment

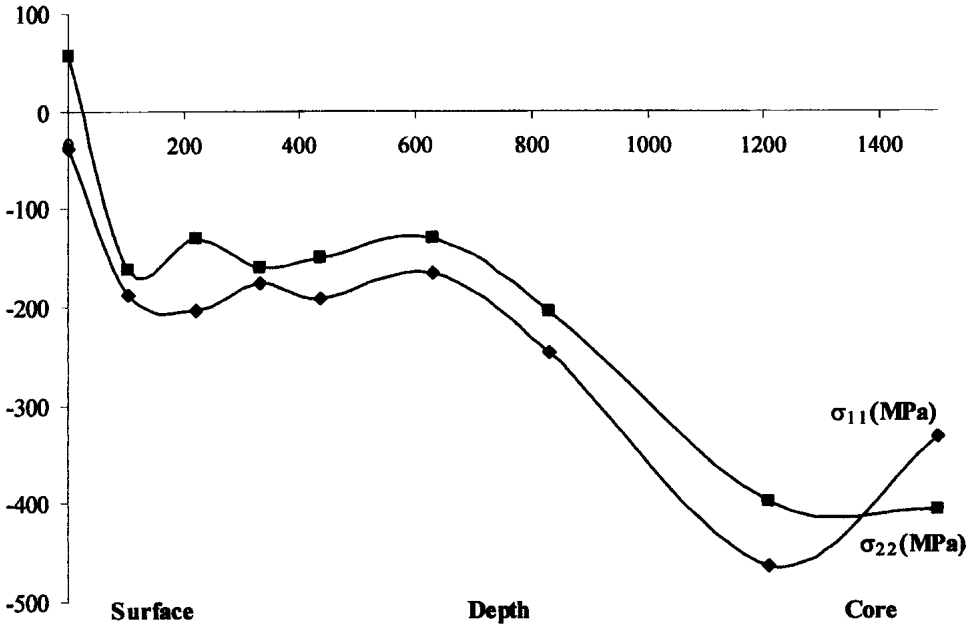

Fig. 8 Residual stress profiles generated by type 2 treatment

dation layer thickness. The analyzed microstructure is thus a mixture of retained austenite and martensite in proportions that depend on the point of measurement.

4.3 Residual Stresses

The profiles of the residual stresses measured at the bottom of the specimen notch in two directions show compressive stresses in layers adjacent to the surface at a depth of 1 mm, or greater, for both types of carburizing treatments (Fig. 7, 8). These profiles mark plateaus around −400 MPa for the type 1 treatment and −200 MPa for the type 2 treatment (at depths between 100 and 600 μm, or slightly deeper). Stresses on the upper surface were measured for the two types of treatments and can be attributed to the role of internal oxidation as highlighted in this study.

4.4 Fatigue Strength of Carburized Layer

Test results of four-point bend fatigue tests of untreated and carburized notched samples according to two types of treatments are plotted on Wöhler diagrams (Fig. 9). Endurance limits $\Delta\sigma_D = (1 - R)\,\sigma_{max}$, where $\sigma_{max} = K_T\,\sigma_{nom}$, are given for 10^6 cycles by the staircase method, and the rates of im-

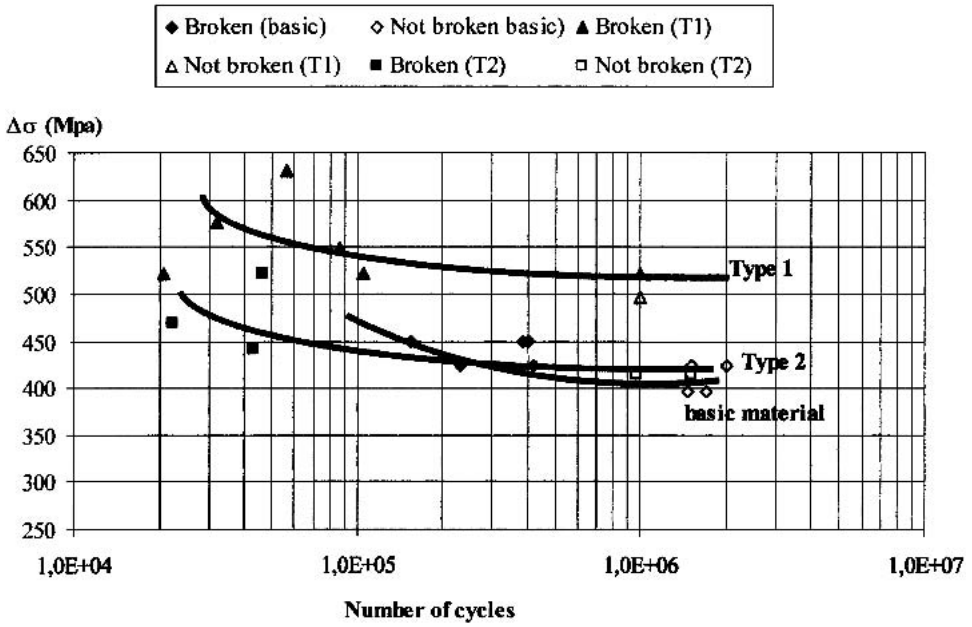

Fig. 9 Wöhler diagrams corresponding to the two types of treatments compared with that of basic material

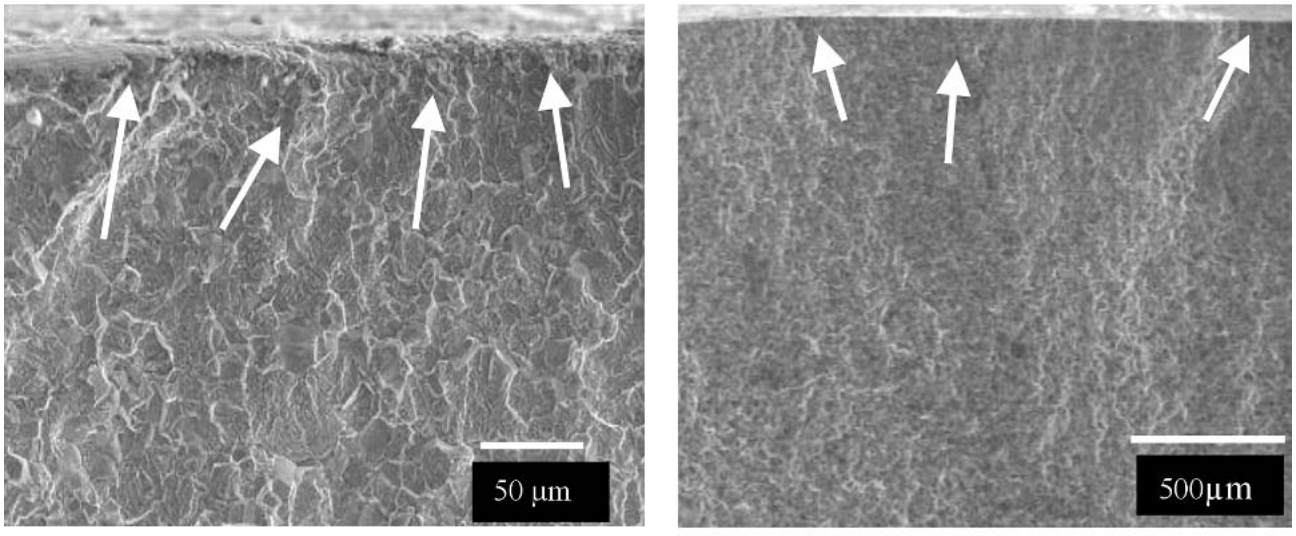

Fig. 10 Multiple crack initiation on the upper surface

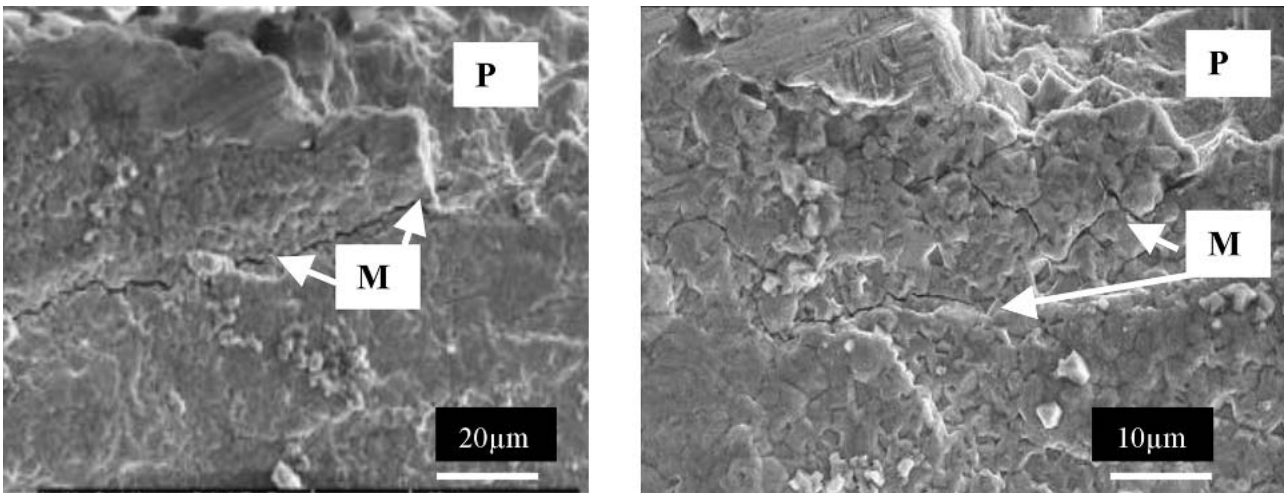

Fig. 11 Microcrack coalescence and principal rupture (type 1: σ_{max} = 610 MPa, N_r = 86,890)

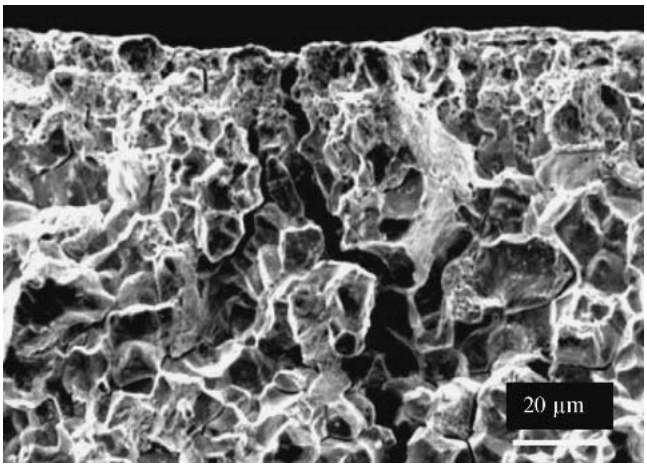

Fig. 12 Intergranular initiation (type 1: σ_{max} = 610 MPa; N_r = 86,890)

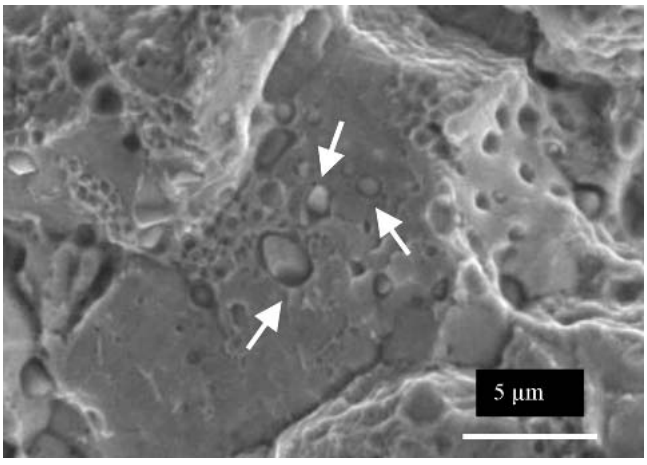

Fig. 13 Facets of the grains sprinkled with various sized particles, ranging between 0.5 and 2 μm (type 1: σ_{max} = 610 MPa; N_r = 86,890)

provement resulting from both types of treatment, $(\Delta\sigma_{Dtreated} - \Delta\sigma_{Dbasic})/\Delta\sigma_{Dbasic}$, are given in Table 4. The standard deviation could not be estimated given the limited number of samples.

4.5 Microfractographic Analysis

4.5.1 Crack Initiation. Microfractographic analysis, under low magnification of the fracture surfaces of the two treated states, shows different fracture mechanisms. The treated layers can be distinguished from the core material. Crack initiation is at the surface at the bottom of notch (i.e., the site of the stress concentration) (Fig. 10).

Inspection of the fracture surface at the bottom of the notch using SEM confirms that the crack-initiation mechanism is characterized by the formation of microcracks on the surface in various planes (letter "M" on Fig. 11). These microcracks coalesce to form a macroscopic crack that is responsible for the principal fracture (letter "P" on Fig. 11).

With higher magnification, the microfractographic examinations show that intergranular cracks are favored, and start by internal oxidation and the intergranular carbide precipitation (Fig. 12). Indeed, the facets of the grains appear sprinkled by various sized particles (Fig. 13).

4.5.2 Crack Propagation. The general aspect of the fracture surface shows progressive brittle fatigue crack propagation in the type 1 and 2 treated layers (Fig. 14). The brittle character of this fracture is attributed to intergranular rupture at the surface, which gradually shifts to transgranular fracture in the underlayers (Fig. 14). Fatigue striations are observed only at the interface between the treated layer and the bulk material (Fig. 15).

4.6 Stability of Retained Austenite After Loading

To understand the effect of the retained austenite on fatigue strength, measurements of the phase fraction by XRD were taken at the surface and at a depth of 200 μm, before and after cyclic loading, at a maximum applied stress equal to 85% of the endurance limit. The measurements highlight the instability

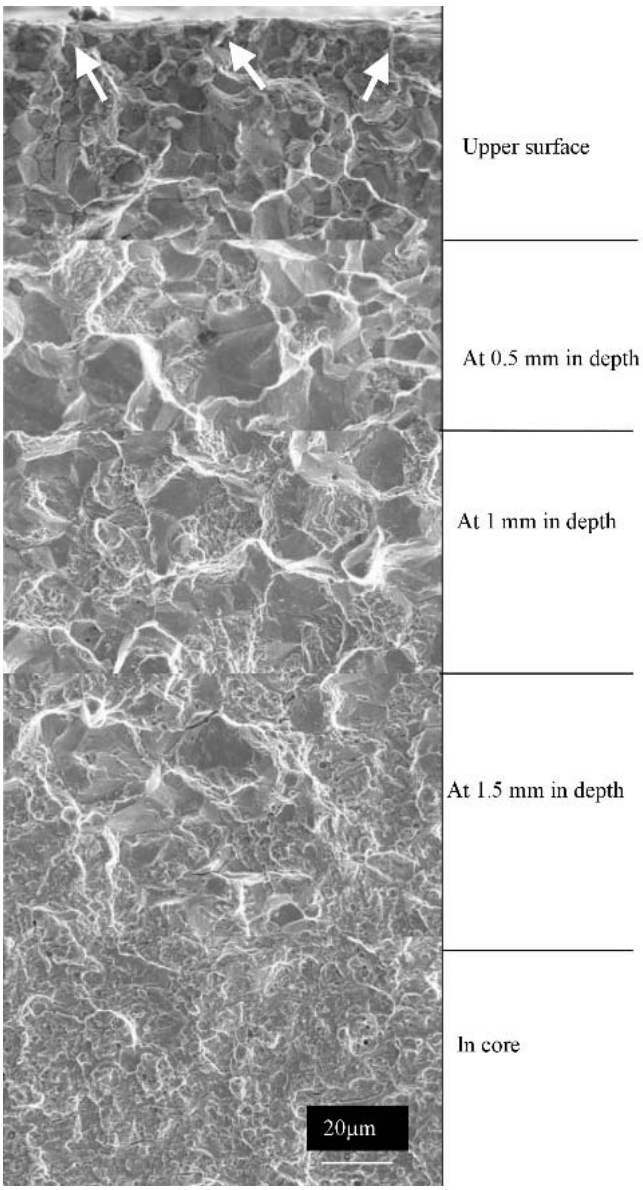

Fig. 14 Microfractograph of gradient fracture surface treated according to type 1: σ_{max} = 610 MPa; N_r = 86,890

of retained austenite with respect to the cyclic loading condition for both treatments (Fig. 16, 17).

Qualitatively, this instability is more significant for austenite from the type 1 treatment than for austenite from the type 2 treatment. Indeed, after 10^6 cycles at a maximum applied stress of 490 MPa, the fraction of transformed retained austenite remains relatively constant up to a depth of 200 μm, and it is about 40% of the initial fraction. For the type 2 treatment, the fraction of transformed retained austenite is more significant with depth, and it goes from 18% at the surface to 35% at a depth of 200 μm after 10^6 cycles at an applied maximum stress of 390 MPa. In all cases, the retained austenite fraction remained higher for the type 2 treatment (25%) than for the type 1 treatment (14.5%) after 10^6 fatigue cycles.

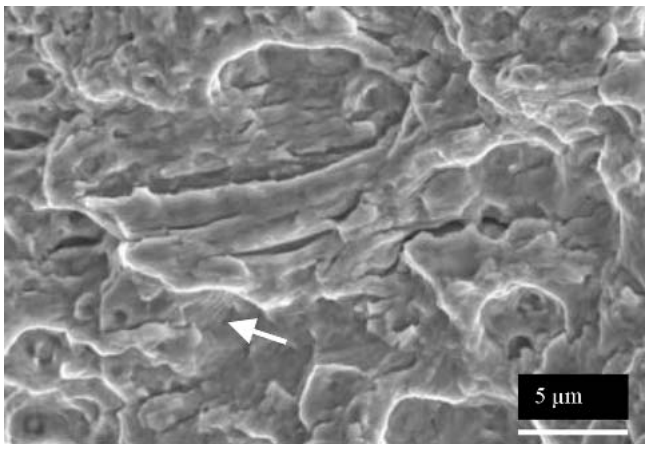

Fig. 15 Fatigue striations (type 1: σ_{max} = 610 MPa; N_r = 86,890)

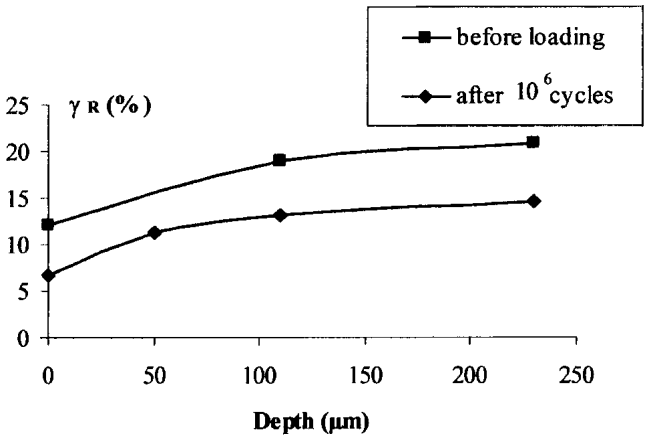

Fig. 16 Evolution of retained austenite faction during cyclic loading with σ_{max} = 490 MPa, in the case of type 1 treatment

5. Discussion

The results of this study showed that improvements in the fatigue life of 14NiCr11 steel, subjected to the two carburizing treatments (10 and 40%), are closely related to the microstructural characteristics of the hardened layers and are controlled primarily by the retained austenite fraction and its evolution during cyclic loading.

5.1 Surface Hardening

Although the two heat treatments developed different retained austenite fractions (20% for type 1 and 40% for type 2), the surface hardness and the treated layer depths are comparable for both treatments. This is probably due to significant C supersaturation of the retained austenite in the surface layers, which gives it an intrinsic hardness comparable to that of martensite.

On the surface, the tendency of the alloy to soften is explained by the internal oxidation phenomenon. It caused the low local C content responsible for the retained austenite fraction reduction and the C supersaturation in the austenite and

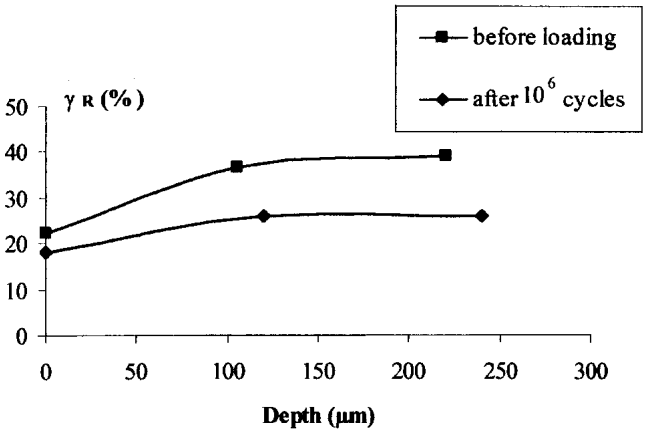

Fig. 17 Evolution of retained austenite faction during cyclic loading with σ_{max} = 390 MPa in the case of type 2 treatment

martensite to decrease (Ref 2, 44, 54, 56-58). In all cases, the treated layer depths obtained by the type 1 and type 2 treatments are common in industrial practice and softening due to internal oxidation remains within acceptable tolerance limits (Ref 2, 59-66).

5.2 Residual Stresses

Due to its C gradient, the carburized layer can be compared with the juxtaposition of steels with different C contents and cooling laws (Ref 67). This implies that phase transformations between layers will be delayed. This is confirmed by volume change effects associated with the $\gamma \rightarrow \alpha$ transformation and the distribution of the compressive residual stresses. For this reason, the type 1 treatment with a higher $\gamma \rightarrow \alpha$ transformation rate (γ_R = 20%) has a residual stress approaching –400 MPa, whereas the type 2 treatment with (γ_R = 40%) exhibits a lower compressive residual stress (–200 MPa).

The close relationship between the martensitic transformation and residual stress can be clearly visualized by the superposition of the retained austenite and the residual stresses profiles (Fig. 18). This superposition explains the difference between the two types of carburizing treatments. The direction of decreasing retained austenite is also the direction of increasing compressive residual stress. Analytical relations (σ_R-γ_R) can be obtained expressing the amplitudes of residual stress (σ^R_{max}) in terms of the retained austenite fraction after the gas-carburizing treatment (Fig. 19):

$$\sigma_R = 297.13\ ln\ (1 - \gamma_R) - 1265$$

based on the relation of Köstinen and Marburger, $V_\gamma = e^{-0.01(M_S-25)}$. This relation gives the retained austenite fraction as V_γ. A relation between the residual stress (σ_R) and the martensitic transformation start temperature (M_S), can be established:

$$\sigma_R = -2.9713M_S + 164.29$$

(Fig. 20). Using the relation given by Steven and Haynes

$$M_S = 561 - (474)C - (33)Mn - (17)Ni - (17)Cr - (21)Mo$$

which expresses M_S as a function of the steel chemical composition. It now becomes possible to establish the relationship between residual stress and C content (%C) as σ_R = (1407.4)C – 1241.7 (see Fig. 21). This relation is extremely useful for gas-carburizing treatments.

5.3 Fatigue Strength

The calculated endurance limits of carburized 14NiCr11 steel for both treatments are within the accepted limits of data for gas-carburized steel with microstructural treated layers similar to the present case, namely, an internal oxidation layer (≤15 μm) and a maximum retained austenite fraction between 20% and 30% (Table 5).

The fatigue strength of carburized 14NiCr11 steel was improved by 40% for the type 1 treatment and 10% for the type 2 treatment, compared with the fatigue strength of the untreated steel. These improvements correspond to 20 and 40% maximum retained austenite fractions, respectively.

This difference in fatigue strength improvement between both gas-carburizing treatments can be explained by the role of the microstructure and residual stress distribution around the crack initiation region. Indeed, microfractographic analysis of the fatigue rupture surface revealed rapid crack propagation after initiation. Taking into account the flattened shape of the Wöhler diagram, an assumption can be made that the crack initiation phase is the main contributor to the fatigue life. This crack initiation can be attributed, in major part, to the microstructural characteristics and the residual stress distribution of the upper surface layers (≤200 μm), as summarized in Table 6.

In these surface layers, the microstructure and the compressive residual stress distribution give an advantage to the type 1 treatment rather than the type 2 treatment. This results in a more significant improvement in its fatigue strength. Moreover, this advantage is consolidated by the retained austenite fraction that evolved during cyclic loading and its effects on the deformation located in the surface upper layers (≤200 μm). Indeed, retained austenite measurements before and after cyclic loading reveal that the transformed fraction of retained austenite for the type 1 treatment is constant at around 40% at any depth. The corresponding layer is, thus, subjected to identical deformations at any point. The transformed retained austenite fraction for the type 2 treatment varies with depth (i.e., from 18 to 35%). The corresponding layer is then subjected to significant deformation, which probably has an adverse role on its fatigue strength.

6. Conclusion

The two types of gas-carburizing treatments generate microhardness and residual stress changes that are strongly related to the retained austenite fraction in the microstructure. The fatigue strength improvement of carburized 14NiCr11 steel compared with its untreated state is close to 40% for the type 1 treatment and 10% for the type 2 treatment. These correspond to maximum retained austenite fractions of 20%

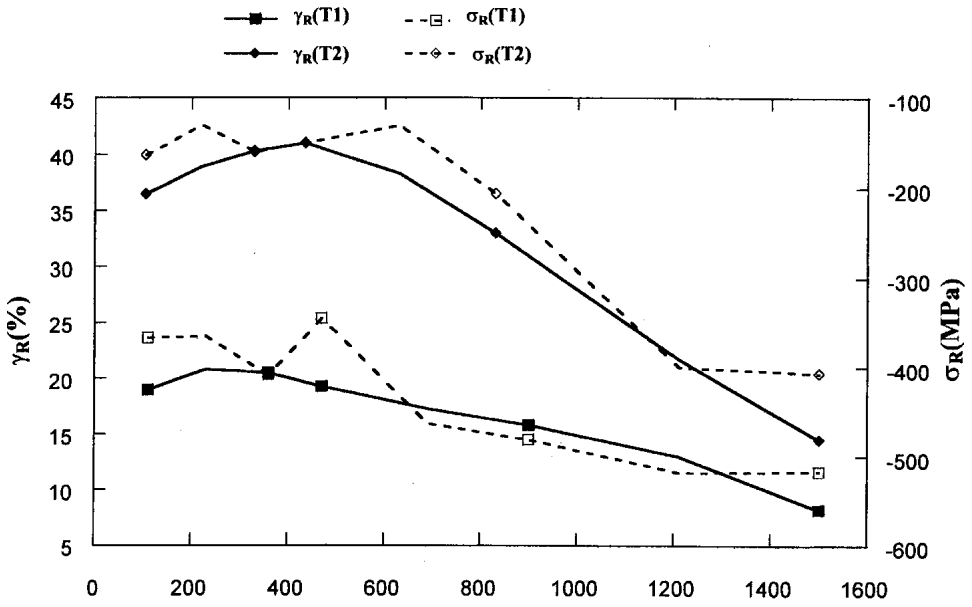

Fig. 18 Comparison of the profiles of residual stress and retained austenite of type 1 (T1) and type 2 (T2) treatment

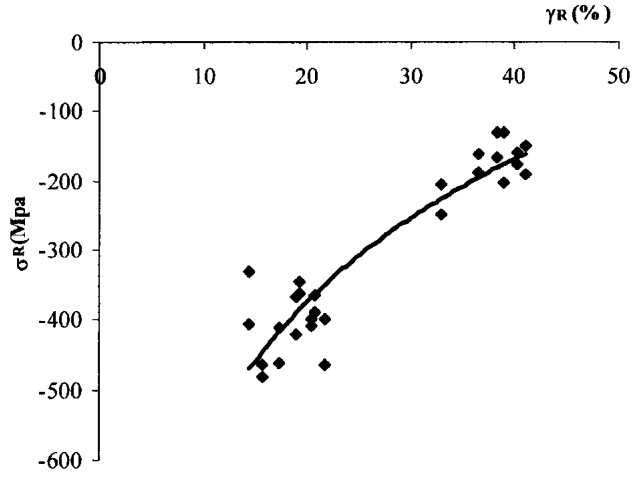

Fig. 19 Curve representative of the experimental points expressing the relationship between residual stress and retained austenite

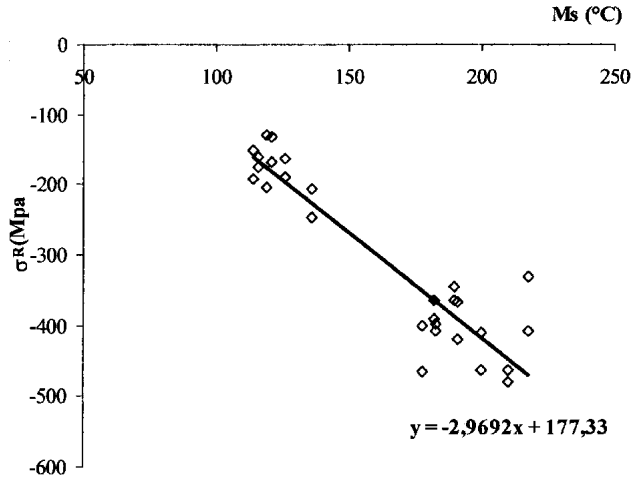

Fig. 20 Relationship between σ_R and M_S

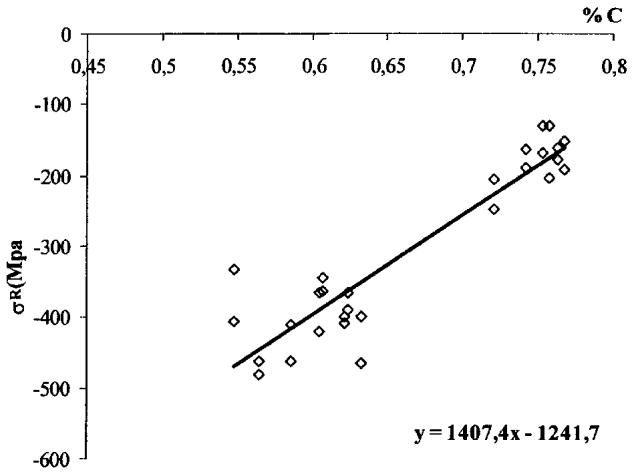

Fig. 21 Relationship between σ_R and the percentage of C

Table 5 Endurance limits

Treatment	$\Delta\sigma_D$, MPa(a)	Improvement, % $(\Delta\sigma_{Dtreated} - \Delta\sigma_{Dbase})/\Delta\sigma_{Dbase}$
Basic material	670	0
Type I	930	40
Type II	740	10

(a) $\Delta\sigma_D = K_t\Delta\sigma_{nom}$

and 40%, respectively. This gain in fatigue strength can be attributed to:

- The type 1 treatment generates a microhardness and compressive residual stress higher than those obtained from the type 2 treatment.

Table 6 Role of microstructure on bending fatigue strength of carburized steels

Ref	Steel grade	Treatment parameters			Microstructure of treated layer				Fatigue data			
		T, °C	t, min	State	e, mm	γ_R, %	σ_{surf}	Oxided layer depth, μm	K_t	R	$\Delta\sigma_D$, MPa(a)	Improvement, %
23	17CrNiMo06 (1)	930	206	QO 60 °C T 180 °C	1.02	31	−140	10	1.35	−1	764	…
	(2)	930	220	QO 60 °C T 180 °C	0.97	23	−220	7	1.35	−1	888	…
	15CrNi6 (1)	930	261	QO 60 °C T 180 °C	0.84	26	−280	7	1.35	−1	914	…
	(2)	…	300	QO 60 °C T 180 °C	0.82	24	−310	9	1.35	−1	838	…
63	20CD4	930	120	QO and T	0.58	17.1	+17	8.7	…	…	780	…
				180 °C	0.65	19.1	+127	15	…	…	450	…
This study	14NiCr11	920	480	QO 50 °C T 180 °C 1h	1.8	19	+184	12	1.78	0.1	930	40
		950	360	QO 50 °C T 180 °C 1h	2.2	29	+57				740	10

Note: Q, quenched; O, oil; T, tempered. (a) $\Delta\sigma_D = K_t\Delta\sigma_{Dnom}$

Table 7 Summary of data in the upper surface/at a depth of 200 μm from the upper surface

Type of treatment	$Hv_{0.1}$	γ_R, %	σ_{11}, MPa	σ_{22}, MPa	$\Delta\sigma_D$, MPa	Improvement, %
Type 1	747/733	12/20	−71/−390	184/−365	930	40
Type 2	718/696	22/40	−39/−203	57/−130	740	10

Note: γ_R, retained austenite; σ_{11}, transverse residual stress; σ_{22}, longitudinal residual stress; $\Delta\sigma_D$, endurance limit

- Internal oxidation not exceeding 12 μm in depth for the two treatments plays a weak role in the fatigue strength of carburized 14NiCr11 steel.

The retained austenite is unstable during cyclic loading. The transformed fraction compared with the unloaded state depends on the type of treatment and can reach 40%. The best fatigue strength is attained when homogeneous transformation of the retained austenite fraction occurs in the treated layer during the cyclic loading.

References

1. H.P. Lieurade, Effet des Contraintes Résiduelles sur le Comportement à la Fatigue des Pièces et des Structures Industrielles, *Traite. Therm.,* (No. 216), 1988, p 15-28 (in French)
2. D. Ghiglione and H.P. Lieurade, "Le Rôle des Traitements Thermochimiques sur la Tenue à la Fatigue des Composants Mécaniques," presented at Conference Traitement de Surface et Composants Mécaniques (Troyes, France), Dec 1991 (in French)
3. R. Varol, Effect of Heat and Mechanical Surface Treatments on the Fatigue Properties of SAE 8620 Steel, Societé Françoise de Metallurgie, *Metalli.,* Vol 50 (No. 4), 1996, p 257-259
4. S. Deshayes, J. German, P. Jacquot, E. Denisse, and G. Dervieux, La Cémentation Basse Pression des Aciers, *Traite. Therm.,* (No. 261), 1993, p 27-34 (in French)
5. J. St-Pierre, La Cémentation à Haute Température: Durée des Opérations, *Traite. Therm.,* (No. 255), 1992, p 37-40 (in French)
6. F. Scinatbaum and A. Melber, Plasma Carburizing of Steel in Pulsed Direct-Current Glow Discharge, *Heat Treat. Met.,* (No. 2), 1994, p 45-50
7. M.K. Lei and Z.L. Zhang, Plasma Source Ion Carburizing of Steel for Improved Wear Resistance, *J. Vac. Sci. Technol., A,* Vol 16 (No. 2), 1998, p 524-529
8. P.H. Bilger and P. Collignon, Cémentation Duplex, *Traite. Therm.,* (No. 309), 1998, p 21-23 (in French)
9. D.H. Herring, Vacuum Carburizing Process Parameters, *Adv. Mater. Proc.,* (No. 12), 1994, p 56-59
10. D.H. Herring and G.P. Read, Vacuum Carburizing Developments, *Metallurgia,* Vol 55 (No. 5), 1986, p 169-172
11. R.J. Cunningham, Qualification de la Cémentation Sous Vide pour les Engrenages d'Hélicoptères, *Traite. Therm.,* (No. 236), 1990, p 79-83 (in French)
12. W.J. Ptashnik, Partial Pressure Carburizing: Its Effect on Durability, *Heat Treat.,* 1980, p 38-44
13. T. Holm, Synthetic Heat Treating Atmospheres, *Adv. Mater. Proc.,* (No. 10), 1989, p 45-47
14. A. Galerie, N. Tu, and M. Caillet, Aspects Thermodynamiques de la Cémentation Activée en Caisse: Cas de l'Aluminisation ou de la Boruration du Fer en Cément Fluoré, *Rev. Métall.,* 1988, p 327-335 (in French)
15. E.J. Kubel, Jr., Extending Carburising Process Capabilities, *Adv. Mater. Proc.,* (No. 3), 1990, p 41-48
16. B. Milet, Les Aciers pour Cémentation, *Traite. Therm.,* (No. 213), 1987, p 25-28, in French
17. L.J. Ebert, The Role of Residual Stresses in the Mechanical Performance of Case Carburized Steels, *Metall. Mater. Trans. A,* Vol 9A, 1978, p 1537-1551
18. G. Parrish, The Influence of Microstructure on the Properties of Case-Carburised Components: Part 6, *Heat Treat. Met.,* (No. 2), 1977, p 45-54
19. H.J. Kim and Y.G. Kweon, High Cycle Fatigue Behavior of Gas-Carburized Medium Carbon Cr-Mo Steel, *Metall. Mater. Trans. A,* Vol 27A, 1996, p 2557-2564
20. E. Szpunar and J. Bielanik, Influence of Retained Austenite on Propa-

gation of Fatigue Cracks in Carburized Cases of Toothed Elements, *Heat Treatment,* Institute of Metals, London, 1984, 85, p 39.1-39.9
21. B. Jeong, M. Kato, K. Inoue, and N. Takatsu, The Bending Strength of Carburized Fine Module Gear Teeth, *JSME, Series III,* Vol 35 (No. 1), 1992, p 136-141
22. G. Parrish, The Influence of Microstructure on the Properties of Case-Carburised Components: Part 4, *Heat Treat. Met.,* (No. 1), 1976, p 6-12
23. M. Larsson, P. Ölund, R. Blom, H. Waburger, A. Melander, and S. Preston, Fatigue Properties After Carburising: Influence of Core Hardness and Notch Geometry on Fatigue Properties of Case Hardened Steels, *Scand. J. Metal.,* Vol 23, 1994, p 62-73
24. G. Krauss, Microstructure and Performance of Carburized Steel: Part II, *Adv. Mater. Proc.,* (No. 7), 1995, p 48U-48Y
25. M.A. Panhans and R.A. Fournelle, High Cycle Fatigue Resistance of AISI E9310 Carburized Steel with Two Different Levels of Surface Retained Austenite and Surface Residual Stress, *J. Heat Treat.,* Vol 2 (No. 1), 1981, p 54-61
26. G. Parrish, The Influence of Microstructure on the Properties of Case-Carburised Components: Part 2, *Heat Treat. Met.,* (No. 2), 1976, p 49-53
27. G. Parrish, The Influence of Microstructure on the Properties of Case-Carburised Components: Part 7, *Heat Treat. Met.,* (No. 3), 1977, p 73-80
28. C. Kim, D.E. Diesburg, and R.M. Buck, Influence of Sub-Zero and Shot-Peening Treatments on Impact and Fatigue Fracture Properties of Case-Hardened Steels, *J. Heat Treat.,* Vol 2 (No. 1), p 43-53
29. A. Yoshida, K. Fujita, T. Kanehara, and K. Ota, Effect of Case Depth on Fatigue Strength of Case-Hardened Gear, *Bull. JSME,* Vol 29 (No. 247), 1986, p 228-234
30. G. Krauss, Microstructure and Performance of Carburized Steel: Part IV, *Adv. Mater. Proc.,* (No. 12), 1995, p 36Z-36DD
31. J. Lesage, D. Chicot, M. Przylecka, and M. Kulka, Rôle du Chrome sur la Cémentation Hyper-Austénitique d'un Acier à Roulement, *Traite. Therm.,* (No. 276), 1994, p 42-46 (in French)
32. K. Asami and H. Emura, Fatigue Strength Characteristics of High-Strength Steel, *JSME, Series I,* Vol 33 (No. 3), 1990, p 367-374
33. M.A. Majid and H.C. Child, Effect of Carburizing on Unidirectional Bending Fatigue Strength of 635 A14 Low-Alloy Steel, *Met. Technol.,* Vol 10, 1983, p 173-181
34. M. Kikuchi, H. Ueda, and T. Naito, Fatigue Behavior of Carburized Steel with Internal Oxides near the Surface, *Metall. Trans. A,* Vol 18A, 1987, p 156-158
35. V.F. Da Silva, L.F. Canale, W.W. Bose-Filho, and O.R. Crnkovic, Influence of Retained Austenite on Short Fatigue Crack Growth and Wear Resistance of Case Carburized Steel, *J. Mater. Eng. Perf.,* Vol 8 (No. 5), 1999, p 543-548
36. W.J. Ptashnik, Partial Pressure Carburizing: Its Effect on Durability, *Heat Treat.,* 1980, p 38-44
37. S. Preston, Influence of Vanadium on the Hardenability of a Carburizing Steel, *J. Heat Treat.,* (No. 8), 1990, p 93-99
38. H. Blumenauer and U. Râcke, Influence of Residual Stresses on Fatigue Crack Growth Behaviour of Case-Hardening Steels, *Third European Conference Residual Stresses,* V. Hauk, H.P. Hougardy, E. Macherauch, and H.-D. Tietz, Ed., Informationsgesellschaft Verlag, Frankfurt, Germany, 1992, p 515-519
39. T.P. Wilks, G.P. Cavallaro, C. Subramanian, K.N. Strafford, and P. French, Conditions Prevailing in the Carburising Process and Their Effect on the Fatigue Properties of Carburised Gears, *J. Mater. Proc. Technol.,* (No. 40), 1994, p 111-125
40. G. Parrish, The Influence of Microstructure on the Properties of Case-Carburised Components: Part 7, *Heat Treat. Met.,* (No. 3), 1977, p 73-80
41. G. Parrish, The Influence of Microstructure on the Properties of Case-Carburised Components: Part 5, *Heat Treat. Met.,* (No. 1), 1977, p 17-27
42. A.G. Goncharov and R.P. Uvarova, Mechanical Properties of Steels After Vacuum and Gas Carburizing, *Metallov. Term. Obrab. Met.,* (No. 5), 1990, p 10-12 (in Russian)
43. G. Krauss, Microstructure and Performance of Carburized Steel: Part III, *Adv. Mater. Proc.,* (No. 9), 1995, p 42EE-42II
44. A. Nakonieczny and W. Szyrle, Residual Stresses, Microstructure and Fatigue Behavior of Carburized Layers Before and After Shot Peening, *Acta Phys. Pol. A,* Vol 89 (No. 3), 1996, p 357-363
45. F. Convert and B. Miege, De Bonnes Raisons de Doser l'Austénite, *Traite. Therm.,* (No. 301), 1997 (in French)
46. M.A. Zaccone and G. Krauss, "Fatigue and Strain Hardening of Simulated Case Microstructures in Carburized Steels," presented at Heat Treatment and Surface Engineering: New Technology and Practical Applications (Chicago, IL), Sept 1998, p 285-290
47. E. Prenosil, Mechanishe Eigenschaften Karbonitrierter Stale: II. Die Dauerfestigkeit Karbonitrierter Stäle, Die Beziehung Zwischen dem Restaustenitgehalt in Karbonitrierten Schichten und der Dauerfestigkeit, *Hart. Tech. Mitt.,* (No. 21), 1966, p 271 (in German)
48. J. Lesage and A. Iost, "Influence de l'Austénite Résiduelles sur la Durée de Vie en Fatigue d'Aciers Carbonitrurés," C.R. Acad. Sc. Paris, t. 305, Series II, Report, Académides Sciences, 1987, p 77-80 (in French)
49. Y. Desalos, Caractérisation vis à vis de la Tenue en Fatigue des Traitements Thermochimiques Utilisés dans l'Automobile, *Traitements et Revêtements de Surface,* Pub. ATT/GAMI CETIM, La Défense-Paris, Dec. 1998, p 1-12 (in French)
50. A. Inada, H. Yaguchi, and T. Inoue, The Effects of Retained Austenite on the Fatigue Properties of Carburised Steels, *Eighth International Congress on Heat Treatment of Materials,* Japan Technical Information Service Tokyo, Kyoto, Japan, 1992, p 409-412
51. B.A. Shaw, F.B. Abudaia, and J.T. Evans, Characterization of Retained Austenite in Case Carburised Gears and Its Influence on Fatigue Performance, *20th ASM Heat Treating Society* (St. Louis, MO), October 2000, ASM International, p 62-69
52. F. Ruckstuhl, M. Martin, and F. Lestrat, Influence du Traitement Thermochimique sur la Mise en Contrainte d'un Matériau par Grenaillage, *ATT95*, Société Française de Métallurgie, Aquaboulevard, Paris, 1995 (in French)
53. B. Criqui, F. Le Strat, M. Frainais, F. Ruckstuhl, C. Hunter, H. Michaud, and C. Pichard, Tenue en Fatigue de Pièces de Pignonnerie Traitées par Trempe de Contour, *ATT96,* Société Française de Métallurgie, Reims, France, 1996 (in French)
54. G. Barreau, P. Ballard, and J. Fournier, Le Choc Laser, *ATT 91*, Société Française de Métallurgie, Toulouse, France, 1991, p 207-219 (in French)
55. F. Convert and B. Miege, Doser Rapidement l'Austénite Résiduelle avec Précision, *ATT96*, Société Française de Métallurgie, Reims, France, 1996 (in French)
56. R. Hoffman and W. Vogel, Cémentation-Trempe Oxydation Marginale Origine, Étendue et Effets, *Traite. Therm.,* (No. 309), 1998, p 30-36 (in French)
57. I.S. Kozlovskii, A.T. Kalinin, A.Y. Novikova, E.A. Lebedeva, and A.I. Feofanova, Internal Oxidation During Case-Hardening of Steels in Endothermic Atmospheres, *Metallov. Term. Obrab. Met.,* (No. 3), 1967, p 2-7 (in Russian)
58. G. Krauss, Microstructure and Performance of Carburized Steel: Part IV, *Adv. Mater. Proc.,* (No. 12), 1995, p 36Z-36DD
59. A. Guimier, Y. Pourprix, and J.F. Flavenot, Influence des Paramètres de Réalisation d'une Couche Cémentée sur la Tenue en Fatigue d'un Acier de Pignonnerie, Fatigue et Traitement de Surface, Société Française de Métallurgie, 1987, p 297-313 (in French)
60. R. Leveque, Définition d'un Traitement Thermochimique en Vue de l'Amélioration de la Tenue en Fatigue, Fatigue et Traitement de Surface, Société Française de Métallurgie, Paris, 1987, p 175-246 (in French)
61. K. Genel and M. Demirkol, Effect of Case Depth on Fatigue Performance of AISI 8620 Carburized Steel, *Int. J. Fatigue,* (Vol 21), 1999, p 207-212
62. A. Nakonieczny, J. Senatorski, J. Tachikowski, G. Tympwski, and W. Lilental, Computer Controlled Gas Nitriding: A Viable Replacement for Carburizing, *Heat Treat. Met.,* (No. 4), 1977, p 81-88
63. F. Lestrat and M. Lamothe, Oxydation Interne et Troostite Après Traitements Thermochimiques, *ATT 92*, Société Française de Métallurgie, Strasbourg, France, 1992, p 269-283 (in French)

64. D. Chicot and J. Lesage, Etude Microstructurale et Fractographique d'un Acier 20NCD2 Cémenté Rompu en Fatigue, *Traite. Therm.,* (No. 264), 1993, p 43-50 (in French)
65. U. Wyss and K.H. Weissohn, Profil des Teneurs en Carbone et des Duretés dans la Couche Cémentée, *Traite. Therm.,* (No. 242), 1990, p 57-62 (in French)
66. G. Parrish, The Influence of Microstructure on the Properties of Case-Carburised Components: Part 5, *Heat Treat. Met.,* (No. 1), 1977, p 17-27
67. J. Barralis and G. Maeder, in *Précis de Métallurgie,* Nathan, Ed., 1997, Chap. Traitement et Revêtement de Surface, p 158-159 (in French)
68. D.P. Kostinen and R.E. Marburger, A General Equation Prescribing the Extent of the Austenite Martensite Transformation in Pure Iron, Carbon Alloys, and Plain Carbon Steels, *Acta. Met.,* (No. 7), 1959 p 59-60
69. A.G. Haynes, Interrelation of Isothermal and Continuous Cooling Heat Treatments of Low-Alloy Steels and Their Practical Significance, *Heat Treat. Met.,* The Iron and Steel Institute, Special Report 95, 1966, p 13-23